Electronic Supplementary Material (ESI) for ChemComm.
This journal is © The Royal Society of Chemistry 2016

Supporting Information

Porosity in Metal-Organic Framework Glasses

A.W. Thornton,[a] K. E. Jelfs,[b] K. Konstas,[c] C. M. Doherty,[c] A. J. Hill,[c] A. K. Cheetham[d] and T. D. Bennett*[d]

SI-1: Synthesis and Characterization

Pycnometric measurements were performed using a Micromeritics Accupyc 1340 helium pycnometer. The typical mass used was 200 mg, the values quoted being the mean and standard deviation from a cycle of 10 measurements.

1.625 (2) $g.cm^{-3}$ or 4.904 (6) $Zn.nm^{-3}$

Room temperature PXRD data (2θ = 5-30°) were collected with a Bruker-AXS D8 diffractometer using Cu Kα (λ =1.540598 Å) radiation and a LynxEye position sensitive detector in Bragg-Brentano parafocusing geometry.

Thermogravimetric analysis (TGA) was performed using a TA Instruments Q-500 series thermal gravimetric analyser, with the sample (0.7 - 5 mg) held on a platinum pan under a continuous flow of argon gas. TGA curves were obtained using a heating rate of 5 °C/min and up to 800 °C.

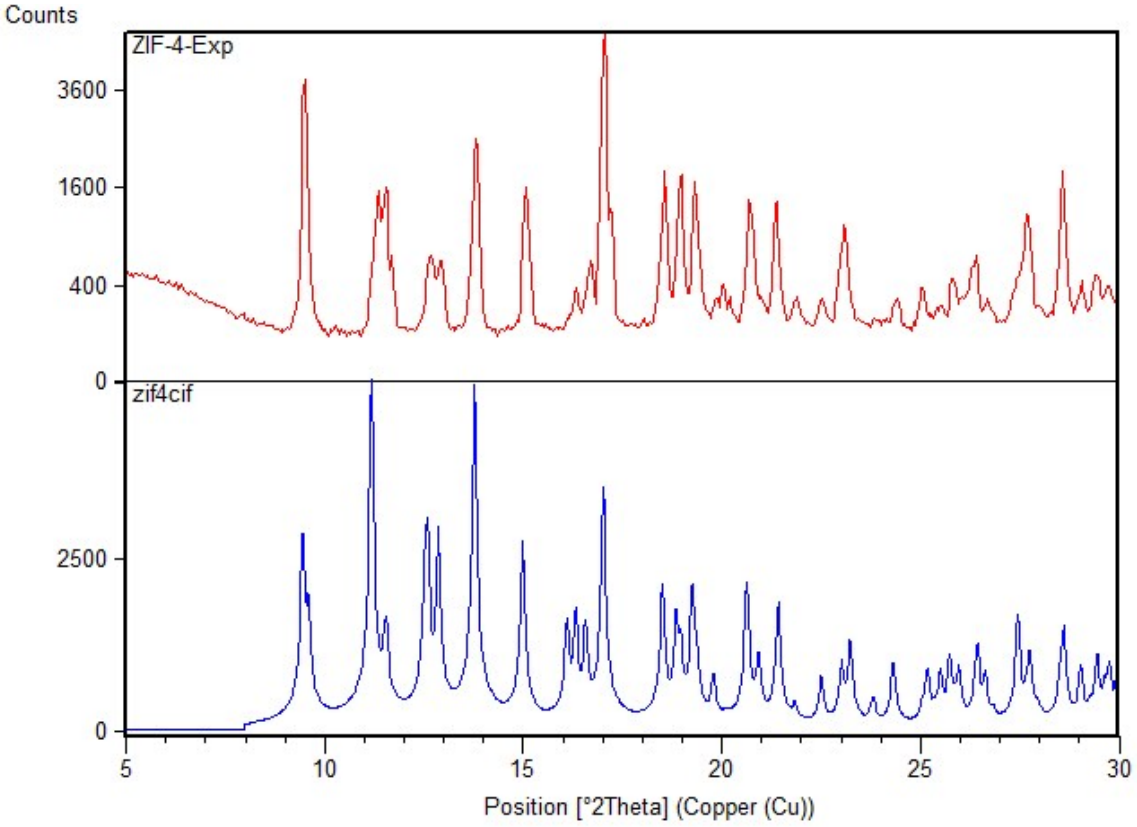
Counts
ZIF-4-Exp
3600
1600
400
0
zif4cif
2500
0
5
10
15
20
25
30
Position [°2Theta] (Copper (Cu))

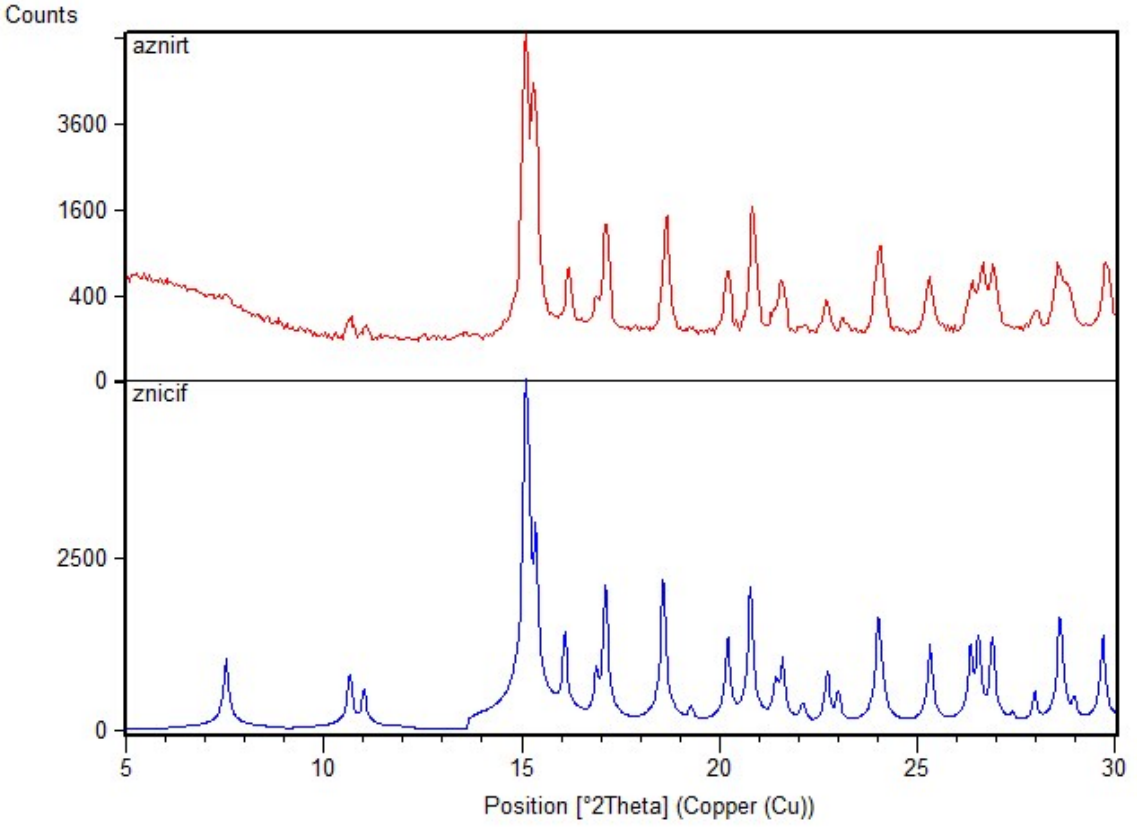
Counts
aznirt
3600
1600
400
0
znicif
2500
0
5
10
15
20
25
30
Position [°2Theta] (Copper (Cu))

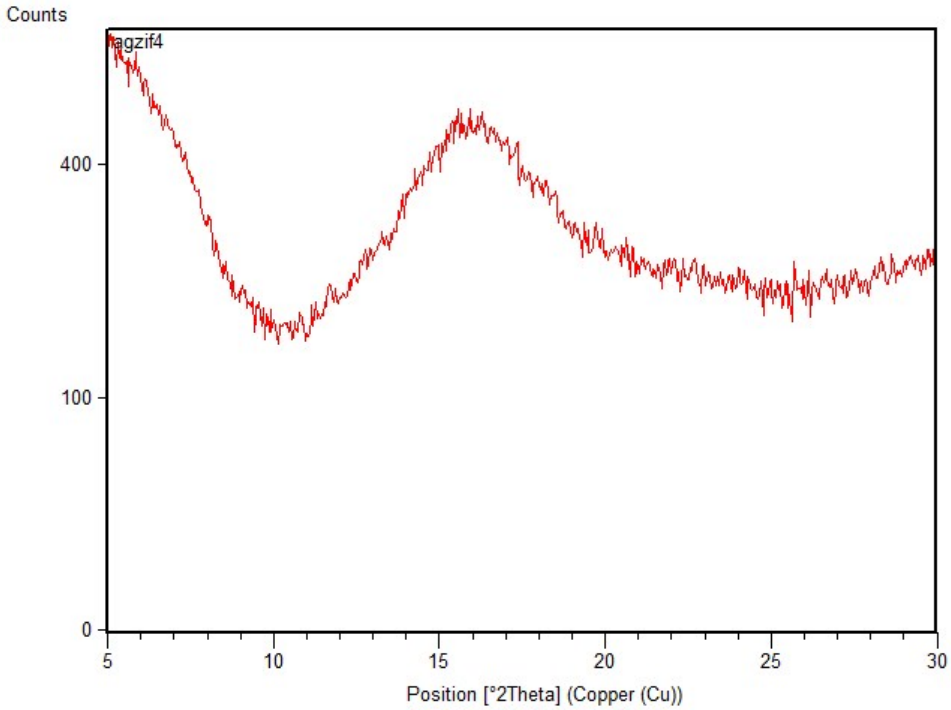

Figure SI-0a: Simulated and experimental X-ray powder diffraction patterns of crystalline ZIF-4 and ZIF-zni, along with a_gZIF-4.

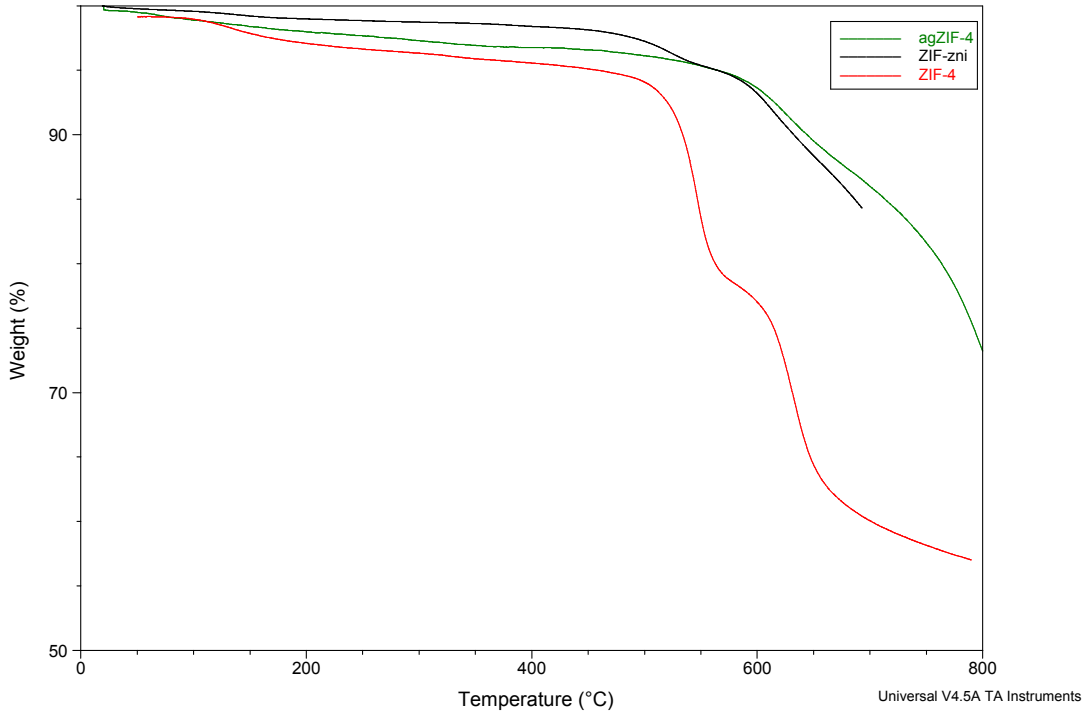

Figure SI-0b: Thermogravimetric analysis of ZIF-4, ZIF-zni and a_gZIF-4.

SI-2: PALS

PALS was used to determine the free volume within the samples by measuring the lifetime of positrons before they annihilate due to interactions with the material. A positron is an anti-particle with the same mass as an electron but positively charged. Positrons can annihilate with electrons in three different ways: 1. Direct annihilation with an electron at a mean lifetime of 0.4 ns, 2. after coupling with an electron of opposite spin forming the particle para-positronium (e^+e^-) at a mean lifetime of 0.125 ns, or 3. After coupling with an electron of identical spin forming the particle ortho-positronium (o-Ps) at a lifetime range of 1 - 140 ns.[1] The o-Ps is attracted to areas of low electron density (free volume) and annihilates when interacting with electrons from the material. Therefore, a relationship between the size of the free-volume elements within the sample can be made with the lifetime of the o-Ps. The longer the lifetimes, the larger the free volume elements within the material. The Tao-Eldrup equation is used to calculate the average free volume size using the o-Ps lifetime (τ),[2, 3]

$$\tau = \frac{1}{2}\left[1 - \frac{R}{R_0} + \frac{1}{2\pi}\sin\left(\frac{2\pi R}{R_0}\right)\right]^{-1} \quad (1)$$

This semi-empirical method assumes an infinite spherical potential well where R is the radius of the free volume element and $R_0 = R + \Delta R$ (where ΔR is 1.66 Å due to the thickness of the electron layer within the potential well of radius R_0). For square infinitely long 2D channels the lifetime is related to the length of the side a, as follows,[4]

$$\tau = 4\left[\lambda_S + 3\lambda_T - (\lambda_S - \lambda_T)\left(1 - \frac{2\delta}{a} + \frac{\sum_{i=1}^{\infty}\frac{1}{i\pi}\sin\left(\frac{2i\pi\delta}{a}\right)e^{\frac{-\beta i^2}{a^2 kT}}}{\sum_{i=1}^{\infty}e^{\frac{-\beta i^2}{a^2 kT}}}\right)^2\right]^{-1} \quad (2)$$

Where λ_S and λ_T are the vacuum decay rates of the singlet and triplet positronium, respectively, δ is the thickness of the electron layer (= ΔR), T is the temperature, k is the Boltzmann factor and β is related to the De Broglie wavelength (= 0.188 eV/nm^2).

The fractional free volume (*FFV*) was calculated assuming spherical free volume elements using the radius determined from the lifetime and the associated intensity (I).

$$FFV_{PALS} = C\frac{4}{3}\pi R^3 I \quad (3)$$

where C is an empirical constant determined to be 0.0018 Å^{-3}.[5]

In this study positrons were formed from the radioactive decay of the ^{22}Na isotope resulting with the formation of a positron and a gamma ray as follows:

$$^{22}_{11}Na \rightarrow ^{22}_{11}Na + e^+ + \gamma(1.28\ MeV)$$

The samples were measured on an EG&G Ortec fast-fast coincidence system using ^{22}NaCl (~1.5 × 10^6 Bq) which was sealed in a thin Mylar envelope. The samples in the form of crystalline powders were packed into a 2 mm thick vacuum cell surrounding the positron source. The measurements were taken under vacuum (1 × 10^{-5} torr) at 298 K collected at 4.5 × 10^6 integrated counts per file for each sample. A source correction of 1.48

ns and 3.033% was subtracted from each spectra. The spectra were deconvoluted using LT v.9 software.[6] Each spectrum was fitted to four components with the first two components fixed to 0.125 ns (para-positronium) and approximated to 0.4 ns (free annihilation). The third and fourth components were due to o-Ps annihilation events indicating the presence of two distinct pore sizes within the materials. Figure SI-1 shows the fit to experimental spectra for all samples. There is excellent agreement between the fitted model and the experimental data. Table SI-1 lists the fitted parameters including o-Ps intensity and lifetime for each sample along with the calculated pore diameters and fractional free volume using Equations 1, 2 and 3.

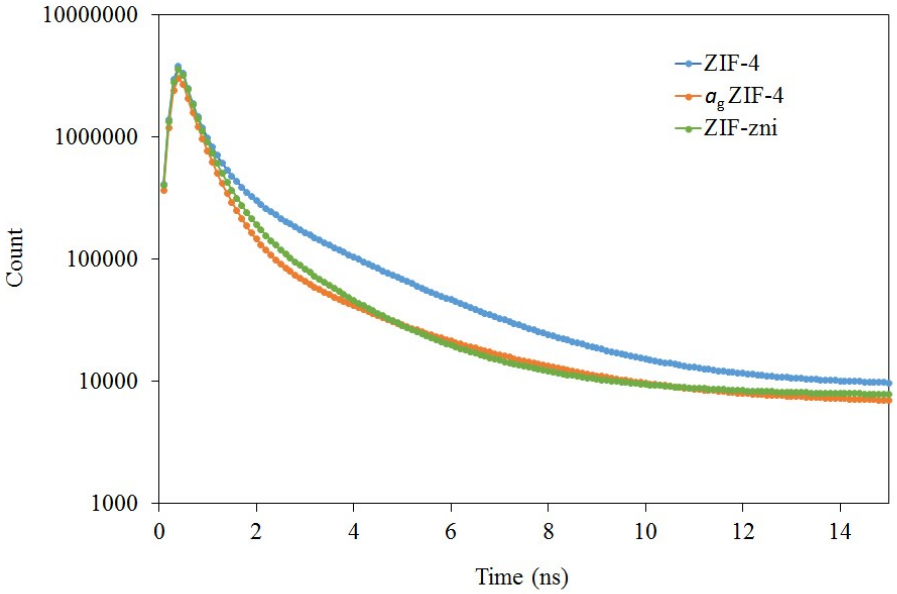

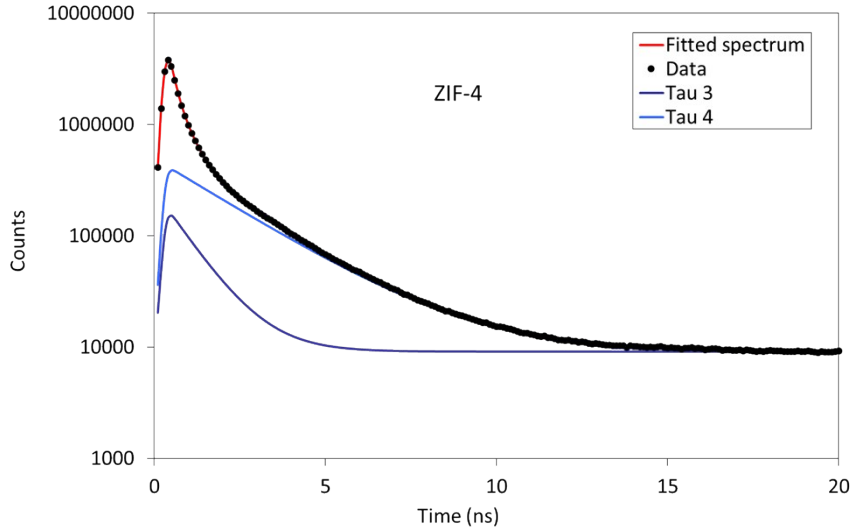

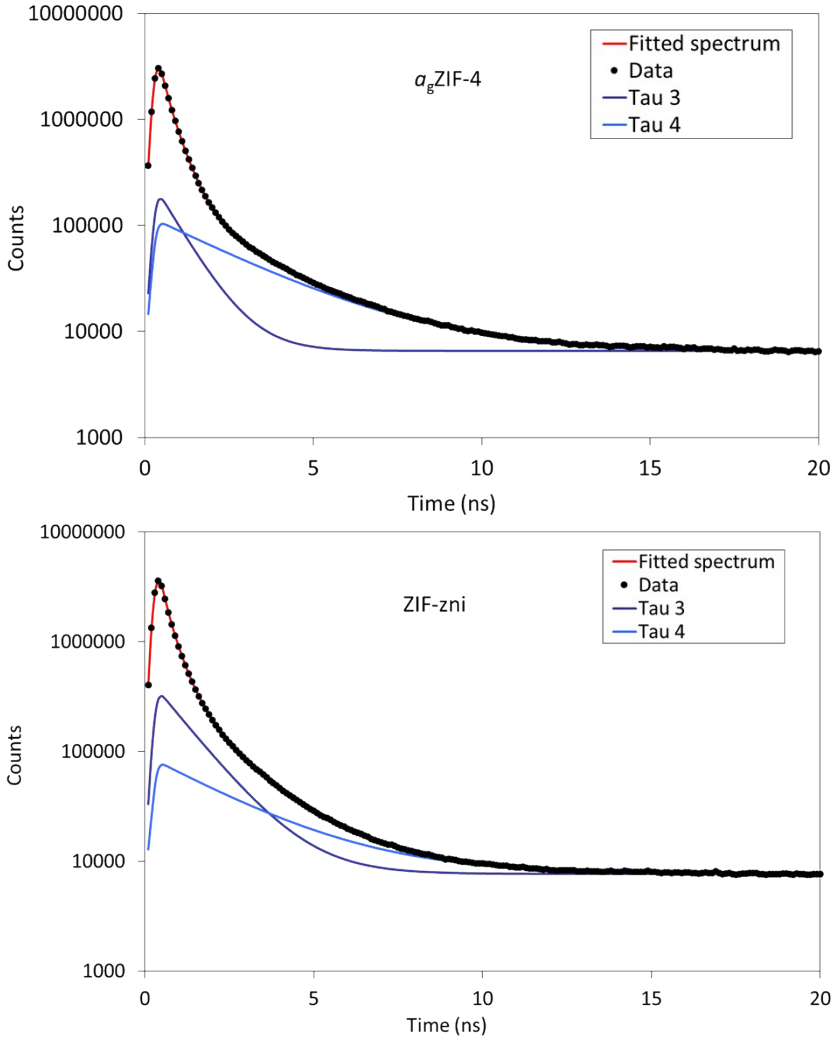

Figure SI-1: PALS results, with number of annihilation events detected at each channel for ZIF-4, a_gZIF-4 and ZIF-zni.

Table SI-1: Fitted parameters for the PALS results with pore size and free volume calculated from Equations 1, 2 and 3.

	Intensity		Lifetime		Pore Size		Free Volume		
Sample	**I_3 (%)**	**I_4 (%)**	**τ_3 (ns)**	**τ_4 (ns)**	**D_3 (nm)**	**D_4 (nm)**	**$FFV_{PALS\ 3}$ (%)**	**$FFV_{PALS\ 4}$ (%)**	**FFV_{PALS} Total (%)**
ZIF-4	6.154 ± 0.631	33.790 ± 1.197	0.981 ± 0.122	2.278 ± 0.012	0.326	0.619	0.20	7.56	7.76
***a*$_g$ZIF-4 glass**	9.134 ± 1.833	14.131 ± 0.269	0.795 ± 0.064	2.706 ± 0.023	0.256	0.686	0.14	4.29	4.43
ZIF-zni	18.266 ± 0.519	7.704 ± 0.972	1.143 ± 0.058	2.527 ± 0.098	0.376	0.659	0.92	2.08	3.00
ZIF-zni*					0.298	0.553	0.46	1.23	1.69

*Assuming square channel geometry from Equation 3.

Table SI-2: Positron annihilation data from the literature.

Material	Pore Number (10^{21} cm^{-3})	Pore Diameter (Å)	Reference
Conventional Polymers			
PVOH poly(vinyl alcohol)	36.97	4.46	Tant *et al.* [7]
PET poly(ethylene terephthalate	27.03	5.02	Tant *et al.* [7]
PBT poly(butylene terephthalate)	28.43	5.14	Tant *et al.* [7]
PCT poly(cyclo hexylene dimethylene terephthalate)	31.74	5.29	Tant *et al.* [7]
PMMA poly(methyl methacrylate)	29.04	5.54	Tant *et al.* [7]
PVAc poly(vinyl acetate)	26.90	5.6	Tant *et al.* [7]
PC poly(bisphenol A carbonate)	29.19	5.72	Tant *et al.* [7]
PAr Poly(arylate)	24.01	5.78	Tant *et al.* [7]
PEU poly(ether urethane)	22.65	6.16	Tant *et al.* [7]
PBMA poly(butyl methacrylate)	22.60	6.28	Tant *et al.* [7]
PPO poly(dimethyl phenylene oxide)	30.14	6.5	Tant *et al.* [7]
PEN poly(ethylene naphthalate)	31.00	4.87	Tant *et al.* [7]
PB Polybutadiene	23.39	6.90	Pejcic *et al.* [8]
PIB Polyisobutylene	24.83	5.95	Pejcic *et al.* [8]
PS Polystyrene	35.01	5.49	Pejcic *et al.* [8]
PSB Polystyrene-co-butadiene	30.74	5.86	Pejcic *et al.* [8]
Polyimide 6FDA-TMPDA	8.41	8.29	Chen *et al.* [9]
sulfonated styrenic pentablock copolymer	13.08	5.96	Geise *et al.* [10]
SW30 Polyamide	6.01	5.14	Lee *et al.* [11]
PMMA film	4.64	6.14	Pejcic *et al.* [12]
PIB film	5.08	6.35	Pejcic *et al.* [12]
PDMS Polydimethylsiloxane	19.10	8.05	Berean *et al.* [13]
Hybrid PVA, maleic acid & TEOS	20.08	5.56	Xie *et al.* [14]
Cellulose acetate 51.6 % acetylation (CDA) and 61.6%(CTA)	19.02	6.01	Chen *et al.* [15]
Cellulose acetate 61.6 % acetylation (CTA)	20.06	6.08	Chen *et al.* [15]
EDE/PDMS Block co-polymers	12.19	4.11	Petzetakis *et al.* [16]
Liquid Crystalline Polymers			
LCP1	16.72	4.8	Tant *et al.* [7]
LCP2	16.58	4.76	Tant *et al.* [7]
LCP3	15.83	4.66	Tant *et al.* [7]

HBA/HNA 73/27 mol% p-hydroxy benzoic acid / hydroxy-2-napthoic acid Vectra	18.75	4.12	Tant *et al.* [7]
HIQ-40 nematic 40 mol% HBA / 30mol% isophthalic acid / 30 mol% hydroquinone	16.44	4.78	Tant *et al.* [7]
PAN Poly(acrylonitrile)	16.76	5.23	Tant *et al.* [7]
HIQ-40 isotropic 40mol% HBA / 30mol% isophthalic acid / 30 mol% hydroquinone	16.97	5.34	Tant *et al.* [7]
Hiq40 LCP	19.39	4.62	Tant *et al.* [7]
Thermally Rearranged Polymers			
TR-1-350	0.60	7.44	Park *et al.* [17]
TR-1-400	1.75	8.36	Park *et al.* [17]
TR-1-450	1.13	9.73	Park *et al.* [17]
High Free Volume Polymers			
PIM-1	2.31	16	Budd *et al.* [18]
PTMSP	7.06	12.38	Staiger *et al.* [19]
AF1600	5.98	9.6	Staiger *et al.* [19]
AF2400	4.17	10.19	Staiger *et al.* [19]
PMP	6.98	11.58	Staiger *et al.* [19]
Zeolitic Imidazolate Frameworks			
ZIF-4	28.06	6.19	This work
ZIF-4 glass	9.57	6.86	This work
ZIF-zni	5.65	5.53	This work
Zeolites and silica			
MFI30	0.94	11.1	Zhu *et al.* [20]
MFI100	1.72	10.5	Zhu *et al.* [20]
MFI500	2.42	11	Zhu *et al.* [20]
High silica MFI	4.38	10.6	Zhu *et al.* [20]
MFI Silicalite	5.27	10.5	Zhu *et al.* [20]
Metal-Organic Frameworks			
HKUST-1	1.52	9.7	Liu *et al.* [21]
MOF-5	1.84	15	Liu *et al.* [21]
MIL-101	0.44	12	Jeazet *et al.* [22]
PAF-1	0.60	12.2	Konstas *et al.* [23]
PAF-1 with 5% Li	2.20	10.6	Konstas *et al.* [23]

SI-3: Simulation

The amorphous glass structure of a_gZIF-4 was simulated using Polymatic, a generalized polymerization algorithm for amorphous polymers.[24, 25] Polymatic was adapted such that multiple bonds could be formed with each zinc atom (up to a maximum of 4). The precursor units, Zn and the imidazole ($C_3H_2N_2$), were randomly loaded in a 1 Zn: 2 ($C_3H_2N_2$) ratio within a 125 x 125 x 125 Å cell with periodic boundary conditions applied at an artificially low density of 0.3 g/cm^3. The approach then searches for reactive end groups within a 6 Å cut-off. This is iterated with equilibration and Molecular Dynamics (MD) steps using the LAMMPS software package. This is continued until all bonds are formed or until no pair meeting the bonding criteria is identified. The force fields used here was adapted from that of Hu *et al.* for ZIF-8, with the only difference being that the charges were modified for overall charge neutralisation to Zn (+0.6894), N (-0.2800), C1 (+0.1618), C2 (-0.1910), H1 (+0.1283) and H2 (+0.1536), where nomenclature is as per Hu *et al.*[26] A total of 5 independent structures were simulated to estimate the average bulk properties. Pore size distributions are shown in Figure SI-2 for each model. In this study 98.6% of reactions on average were completed resulting in a total average density of 1.417 (±0.005) g/cm^3 or 4.277 (±0.014) Zn/nm^3 This is remarkably close to the experimental density of 1.625 g/cm^3 or 4.343 Zn/nm^3 measured in this work, considering that there is a 0.2 g/cm^3 error between the perfect crystal density of ZIF-4 and the measured density from pycnometry. Note that this algorithm does not require density as an input, therefore the resulting density is purely an outcome of the dynamics, reactions and equilibration cycle. In addition, the application of a 21-step annealing routine described by Colina *et al.*, which we did not apply here, could be expected to further increase the density by ~10 %.[25]

Pore size distributions were compared with the diameter of N_2 at 3.64 from Breck *et al.*[27]

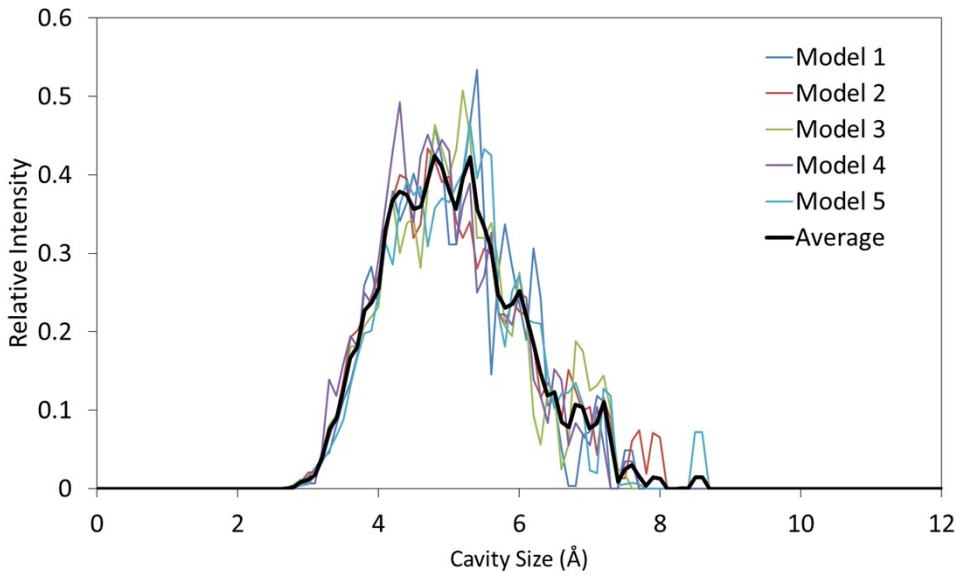

Figure SI-2: Pore size distribution for each independent model of amorphous a_gZIF-4, calculated using *Zeo++*.[28, 29]

References

1. A. J. Hill, I. M. Katz and P. L. Jones, *Polym. Eng. Sci.*, 1990, 30, 762.
2. S. J. Tao, *J. Chem. Phys.*, 1972, 56, 5499-5510.
3. M. Eldrup, D. Lightbody and J. N. Sherwood, *Chem. Phys.*, 1981, 63, 51-58.
4. D. W. Gidley, W. E. Frieze, T. L. Dull, A. F. Yee, E. T. Ryan and H. M. Ho, *Phys. Rev. B*, 1999, 60, R5157-R5160.
5. V. P. Shantarovich, I. B. Kevdina, Y. P. Yampolskii and A. Y. Alentiev, *Macromolecules*, 2000, 33, 7453-7466.
6. J. Kansy, *Nucl. Instrum. Meth. A*, 1996, 374, 235-244.
7. A. J. Hill, M. R. Tant, R. L. McGill, R. R. Shang, D. L. Stockl, D. L. Murray and J. D. Cloyd, *J. Coat. Technol.*, 2001, 73, 115-124.
8. B. Pejcic, E. Crooke, C. M. Doherty, A. J. Hill, M. Myers, X. Qi and A. Ross, *Analytica Chimica Acta*, 2011, 703, 70-79.
9. G. Q. Chen, C. A. Scholes, C. M. Doherty, A. J. Hill, G. G. Qiao and S. E. Kentish, *J. Membr. Sci.*, 2012, 409, 96-104.
10. G. M. Geise, C. L. Willis, C. M. Doherty, A. J. Hill, T. J. Bastow, J. Ford, K. I. Winey, B. D. Freeman and D. R. Paul, *Ind. Eng. Chem. Res.*, 2012, 52, 1056-1068.
11. J. Lee, C. M. Doherty, A. J. Hill and S. E. Kentish, *J. Membr. Sci.*, 2013, 425, 217-226.
12. B. Pejcic, E. Crooke, L. Boyd, C. M. Doherty, A. J. Hill, M. Myers and C. White, *Analytical Chemistry*, 2012, 84, 8564-8570.
13. K. Berean, J. Z. Ou, M. Nour, K. Latham, C. McSweeney, D. Paull, A. Halim, S. Kentish, C. M. Doherty, A. J. Hill and K. Kalantar-zadeh, *Separation and Purification Technology*, 2014, 122, 96-104.
14. Z. Xie, M. Hoang, D. Ng, C. Doherty, A. Hill and S. Gray, *Separation and Purification Technology*, 2014, 127, 10-17.
15. G. Q. Chen, S. Kanehashi, C. M. Doherty, A. J. Hill and S. E. Kentish, *J. Membr. Sci.*, 2015, 487, 249-255.
16. N. Petzetakis, C. M. Doherty, A. W. Thornton, X. C. Chen, P. Cotanda, A. J. Hill and N. P. Balsara, *Nat. Commun.*, 2015, 6.
17. H. B. Park, C. H. Jung, Y. M. Lee, A. J. Hill, S. J. Pas, S. T. Mudie, E. van Wagner, B. D. Freeman and D. J. Cookson, *Science*, 2007, 318, 254-258.
18. P. M. Budd, N. B. McKeown, B. S. Ghanem, K. J. Msayib, D. Fritsch, L. Starannikova, N. Belov, O. Sanfirova, Y. Yampolskii and V. Shantarovich, *J. Membr. Sci.*, 2008, 325, 851-860.
19. C. L. Staiger, S. J. Pas, A. J. Hill and C. J. Cornelius, *Chem. Mater.*, 2008, 20, 2606-2608.
20. B. Zhu, C. M. Doherty, X. Hu, A. J. Hill, L. Zou, Y. S. Lin and M. Duke, *Micropor. Mesopor. Mat.*, 2013, 173, 78-85.
21. M. Liu, A. G. Wong-Foy, R. S. Vallery, W. E. Frieze, J. K. Schnobrich, D. W. Gidley and A. J. Matzger, *Adv. Mater.*, 2010, 22, 1598-1601.
22. H. Jeazet, T. Koschine, C. Staudt, K. Raetzke and C. Janiak, *Membranes*, 2013, 3, 331.
23. K. Konstas, J. W. Taylor, A. W. Thornton, C. M. Doherty, W. X. Lim, T. J. Bastow, D. F. Kennedy, C. D. Wood, B. J. Cox, J. M. Hill, A. J. Hill and M. R. Hill, *Angew. Chem. Int. Ed.*, 2012, 51, 6639-6642.
24. L. J. Abbott, https://nanohub.org/resources/17278, 2013, p. https://nanohub.org/resources/17278.
25. L. Abbott, K. Hart and C. Colina, *Theor. Chem. Acc.*, 2013, 132, 1-19.
26. Z. Hu, L. Zhang and J. Jiang, *J. Chem. Phys.*, 2012, 136, 244703.
27. D. W. Breck, *Zeolite Molecular Sieves: Structure, Chemistry, and Use*, John Wiley & Sons, New York, 1973.
28. M. Haranczyk, C. H. Rycroft, R. L. Martin and T. F. Willems, in *Zeo++: High-throughput analysis of crystalline porous materials* Lawrence Berkeley National Laboratoy, Berkeley, 0.1.0 edn., 2012.

29. T. F. Willems, C. H. Rycroft, M. Kazi, J. C. Meza and M. Haranczyk, *Micropor. Mesopor. Mat.*, 2012, 149, 134-141.